Kirigami-Inspired Flexible Temperature Sensor

May 2, 2025

ADVISOR

Baoxing Xu, Department of Mechanical and Aerospace Engineering

AUTHORS

Annabella Caporaletti

Troy Dodd

Tahmid Mahi

Katrina Shaffer

Sam Thomas

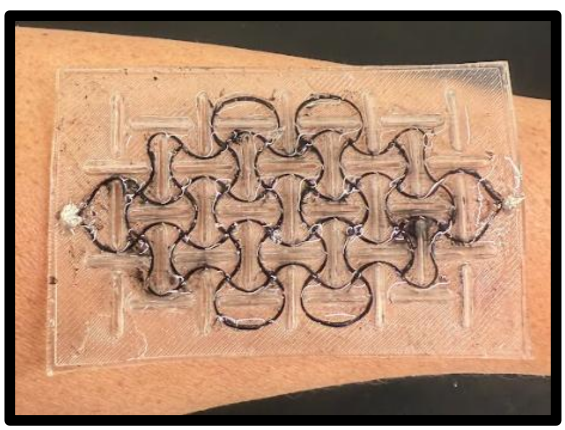

Problem Statement

The goal for our technical project was to design, fabricate, and test a compact, flexible, biocompatible, and stretchable sensor that addresses the shortcomings of traditional medical devices, such as bulkiness, delay of results, and skin irritation. Healthcare innovation focuses on improving patient monitoring and care delivery, with wearable technology providing real-time vital-sign data. Flexible temperature sensors offer continuous, comfortable body temperature monitoring, unlike traditional methods. These sensors are useful for post-operative care, chronic disease management, and geriatric monitoring.

Research

One approach to making a flexible sensor stretchable is incorporating kirigami cuts into the substrate material. Kirigami, a technique involving repetitive paper cutting and folding to create 3D shapes, enables bilateral or unilateral stretching in flexible materials, depending on the pattern used. Won et al. (2019) employed a laser cutter to incise the material, imparting elasticity to their device and allowing it to stretch up to 400%.

Other researchers are developing wearable sensor systems that are flexible, lightweight, and unobtrusive, ensuring comfort, affordability, and long-term wearability. To address design challenges, researchers are exploring novel materials such as printed sensors and flexible electronics to reduce production costs. Carbon-based nanomaterials and metallic nanoparticles are being used to construct sensor electrodes (Nag, 2017). Additionally, efforts are underway to enhance communication networks for efficient data transmission, minimizing delays.

Building on this idea, a study published in *Nature Communications* developed a thin-film material that enhances the mechanical durability of film-based cells and sensors. This material withstands repeated mechanical stresses, making it relevant for our flexible temperature sensors. These sensors benefit from improved reliability and resilience–both crucial for wearable electronics. Given our goal of creating a reusable or long-wearing temperature sensor, this advancement addresses key limitations in conventional temperature sensors, enabling more durable and efficient applications in healthcare and potentially beyond (Yu et al., 2022).

Many wearable technologies address the challenges of medical devices outside of temperature. Abbott's FreeStyle Libre Continuous Glucose Monitor (CGM) became one of the first devices approved by the FDA that allowed diabetic patients to monitor their glucose levels continuously without the need for routine finger stick tests. The FreeStyle Libre, along with other CGMs like Dexcom and Medtronic's Guardian, was hailed as a breakthrough in diabetes management, giving patients real-time data about their glucose levels and enabling better control over their health (Commissioner, 2017). These devices represent a significant shift from traditional methods of glucose monitoring, promising greater convenience and improved health. Despite these advancements, CGMs have encountered several challenges, including issues related to cost, data privacy, and user adaptation (Van Beers & DeVries, 2015).

Ideation

While attempting to come up with the design we would use for our flexible temperature sensor, we considered many ideas, which we list below in Figures 1 through 10.

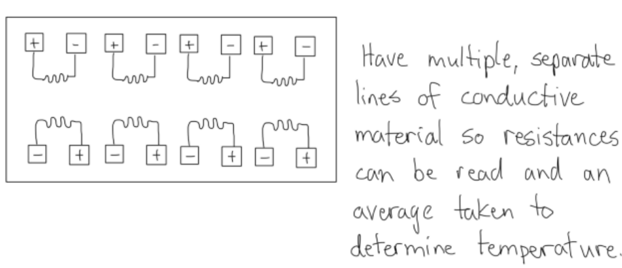

Figure 1: Idea 1

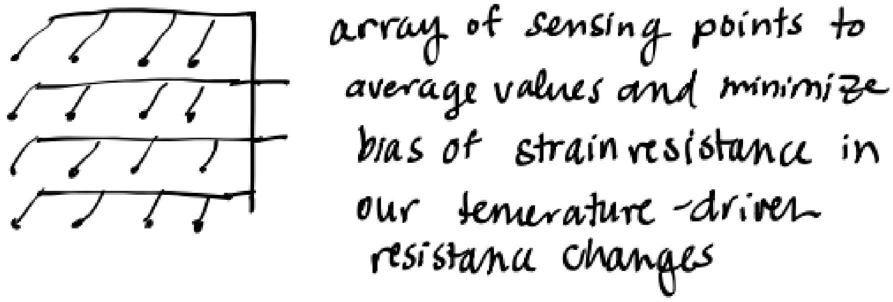

Figure 2: Idea 2

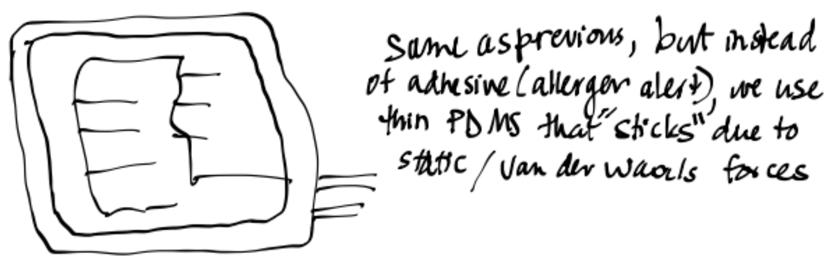

Figure 3: Idea 3

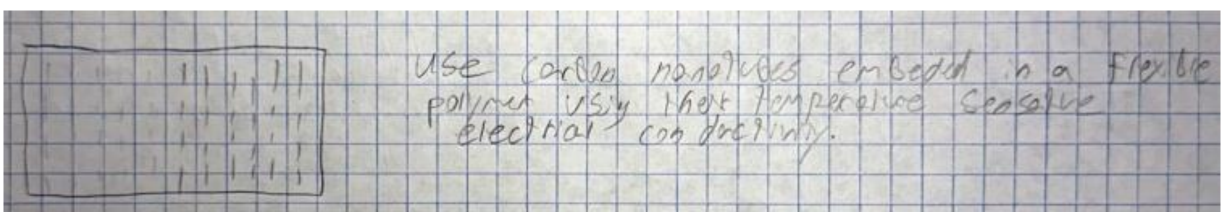

Figure 4: Idea 4

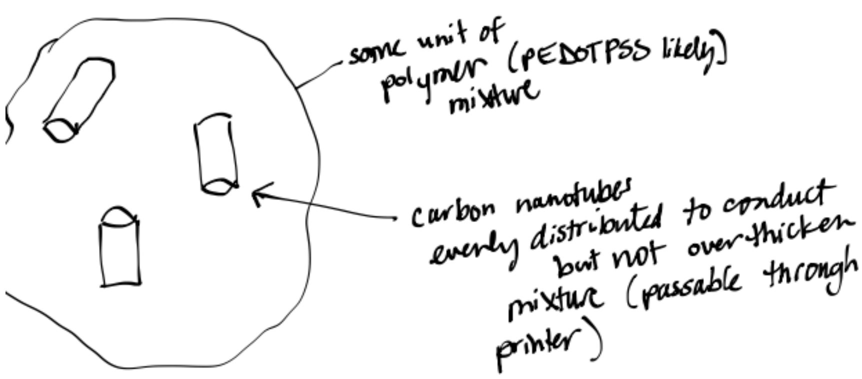

Figure 5: Idea 5

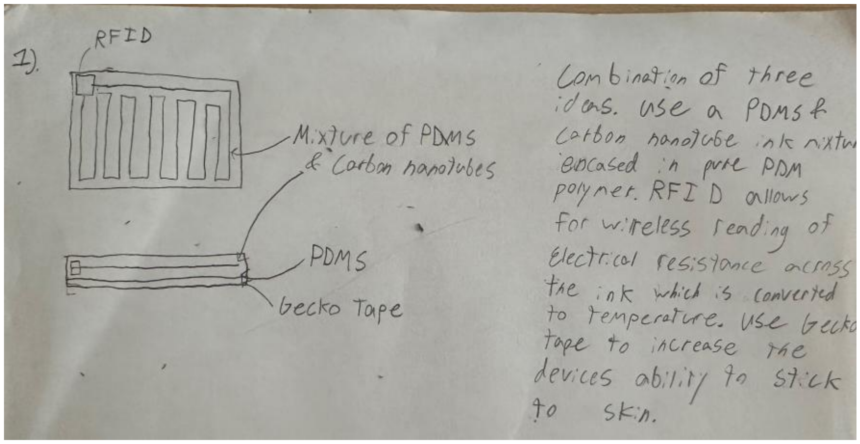

Figure 6: Idea 6

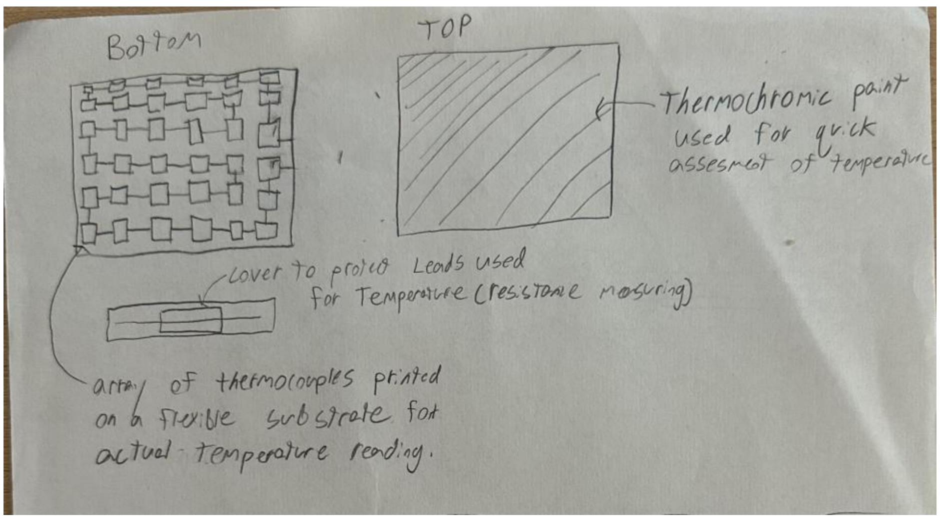

Figure 7: Idea 7

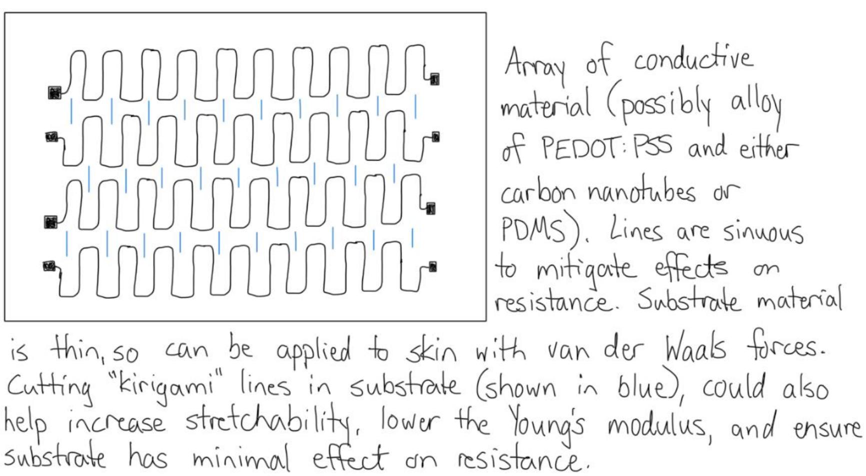

Figure 8: Idea 8

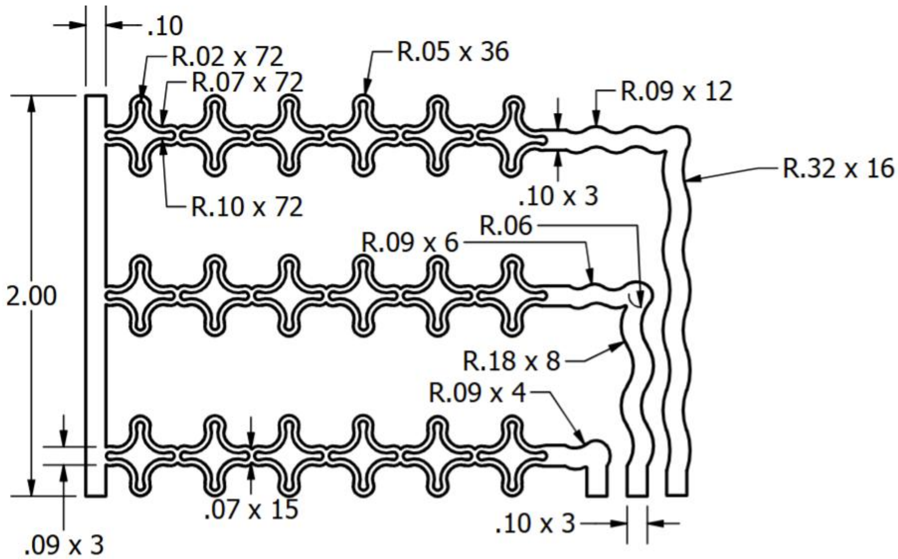

Figure 9: Idea 9. Design of Conductive ink that can withstand deformation in both horizontal and vertical directions with minimal strain. The diamond design allows it to flex in both directions. The design gets in the way of kirigami cuts.

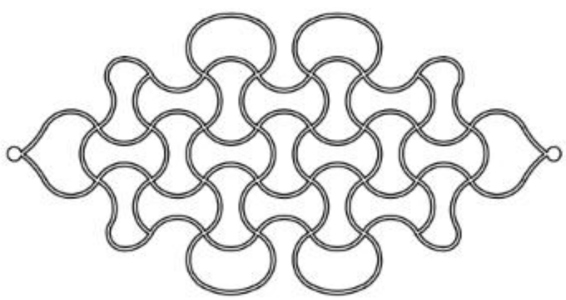

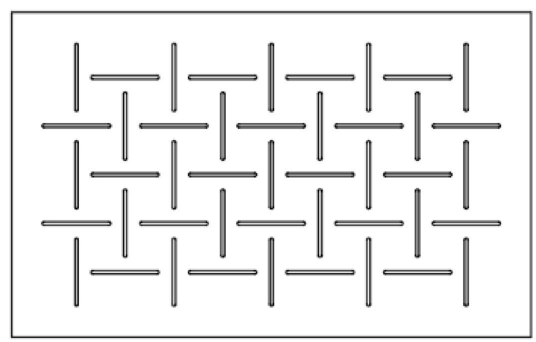

Figure 10: Idea 10. Conductive ink design on the left, with substrate and protective top layer design on the right. The substrate and top layers have kirigami cuts incorporated into them to increase stretchability.

Selection and Screening

Table 1: Idea Selection and Screening

		Concept									
		1		2		3		4		5	
		Rating	Weighted	Rating	Weighted	Rating	Weighted	Rating	Weighted	Rating	Weighted
Flexibility	20%	4	0.8	4	0.8	1	0.2	2	0.4	4	0.8
Sensitivity	20%	3	0.6	4	0.8	0	0	2	0.4	1	0.2
Skin Irritation	5%	5	0.25	1	0.05	4	0.2	1	0.05	0	0
Weight(lighter better)	5%	3	0.15	0	0	4	0.2	3	0.15	2	0.1
Ease of Use	15%	2	0.3	3	0.45	5	0.75	1	0.15	1	0.15
Strain Resistance	20%	1	0.2	4	0.8	3	0.6	5	1	3	0.6
Aesthetically Pleasing	5%	2	0.1	4	0.2	1	0.05	4	0.2	0	0
Wearability	10%	3	0.3	1	0.1	2	0.2	0	0	2	0.2
Total			2.7		3.2		2.2		2.35		2.05
Rank			7		5		9		8		10
Continue?		No		No		No		No		No	

		6		7		8		9		10	
		Rating	Weighted	Rating	Weighted	Rating	Weighted	Rating	Weighted	Rating	Weighted
Flexibility	20%	4	0.8	3	0.6	5	1	5	1	5	1
Sensitivity	20%	4	0.8	4	0.8	5	1	5	1	5	1
Skin Irritation	5%	2	0.1	4	0.2	4	0.2	4	0.2	4	0.2
Weight(lighter better)	5%	3	0.15	3	0.15	4	0.2	4	0.2	4	0.2
Ease of Use	15%	4	0.6	2	0.3	3	0.45	3	0.45	3	0.45
Strain Resistance	20%	3	0.6	2	0.4	4	0.8	4	0.8	5	1
Aesthetically Pleasing	5%	2	0.1	2	0.1	3	0.15	4	0.2	4	0.2
Wearability	10%	3	0.3	2	0.2	3	0.3	4	0.4	4	0.4
Total			3.45		2.75		4.1		4.25		4.45
Rank			4		6		3		2		1
Continue?		No		No		No		No		Yes	

We rated "flexibility," "sensitivity," and "strain resistance" the highest at 20% because they are the most important for achieving our goal and having the product work. We rated "ease of use" the next highest at 15%. Next we had wearability at 10%, because while we can just tape it on to the user, it would be more accepted if that is not needed. Next we rated "skin irritation," "weight," and "aesthetically pleasing" at 5%. While skin irritation is important, we rated it low because any idea that caused a lot of skin irritation would not be usable, so the difference in skin irritation we were comparing between our ideas was low making it matter less. We rated "weight" and "aesthetically pleasing" low because while it would be better for it to weigh less and look good, it is not necessary for the product to work. After our screening process, we decided to proceed with the development of Idea 10 (Figure 10).

Progression of Technical Specifications

Initial Ideation of Specifications

The device we designed was meant to measure skin temperature continuously and transmit data to a smartphone application via contactless method. It was also meant to be used in medical and industrial contexts. This sensor was intended to be flexible, durable, and sterilizable, as well as able to withstand a range of temperatures.

Technical Specifications

The progression of our technical specifications for this continuous skin temperature sensor begins with the core need for accurate temperature readings within the range of 90°F to 105°F. This primary specification directly addresses the fundamental functionality of the device in both medical and industrial contexts. In medical applications, precise temperature monitoring is crucial for detecting fevers, tracking patient recovery, and potentially identifying early signs of infection. Similarly, in industrial settings, continuous temperature monitoring of personnel working in extreme environments can be vital for safety and performance. The methodology for verifying this specification involves calibration tests conducted under controlled temperature environments, ensuring the reliability and accuracy of the sensor's output while being flexed or temperature controlled.

Table 2: Specifications and Importance

Specification	How to Measure	Order of Importance
The sensor must be able to read temperatures between 90°F and 105°F	Perform calibration tests in controlled temperature environments	1
The sensor must be flexible to conform to different body shapes	Apply sensor to various curved objects and human subjects	2
Materials used in sensor must not cause skin irritation or allergic reaction	Check material properties and compare with known materials that cause allergies	3
The sensor must stay on the skin for at least a week	Put the sensor on the object and leave for a week, varying surface conditions. Alternatively, use a human test subject.	4
The product should work reliably in various temperatures and humidities	Place sensor in high and low temp/humidity test environment	5
Device should be able to be sterilized	Petri dish swabs before and after sterilization	6
The materials should cost no more than $15 dollars to produce each sensor	Use cost estimation from different suppliers	7
The product should be able to be disposed of safely w/o harm to environment	Review materials used in fabrication, and check if they can be safely disposed	8
The sensor should transfer data via an NFC and/or wired connection	This is a yes/no specification	9
The sensor should be able to be taken out of package and put on skin in one minute	Time how long it takes to apply product	10

Following the critical need for accurate temperature readings, the flexibility of the sensor to conform to different body shapes is another key aspect of our technical progression. This requirement is particularly vital for ensuring consistent and reliable contact with the skin across anatomical contours in both medical and industrial applications. In healthcare, the sensor might need to adhere comfortably to wrists, arms, or even the forehead, requiring a design that can move with the patient without detaching or causing discomfort. Similarly, in industrial settings, monitoring individuals performing various physical tasks necessitates a flexible sensor that can maintain contact even with movement and bending. The method for measuring this involves applying the sensor to various curved objects and human subjects to assess its ability to conform and maintain adhesion without compromising its functionality. As well as comfort, it's crucial that the sensor flexes without heavily affecting the resistance temperature readings.

Analysis and Calculations

Two technical analyses were performed to test the elasticity of our design. The conductive ink of our temperature sensor needs to stretch 10% in the horizontal direction and 5% in the vertical direction without excessive plastic deformation or, worse, tearing. To help with this, kirigami-based cuts were used in the polydimethylsiloxane (PDMS) substrate layer to reduce the stress felt in the conductive ink. In the first test, a static structural analysis was run using Ansys to determine if it was better to have no cuts or cuts with rounded ends. In our second test, a window cling vinyl was used as a replacement substrate to test the effect of the cuts in a physical manner.

The PDMS substrate with no cuts was tested to determine the amount the sensor would be able to stretch. A biaxial stretch of 10% in the horizontal direction (8 mm) and 5% in the vertical direction (2.5 mm) was applied first to the substrate and conductive ink assembly. The results of this analysis showed the maximum stress occurring in the spaces between the lines for the conductive ink (CNT/PDMS device), as shown in Figure 11. In addition to this, the strain for the sensor was highest in the conductive ink (see Figure 12). Ideally, the substrate would be able to absorb most of the stress so that the conductive ink does not fracture, so cuts will be incorporated into the substrate to allow for this.

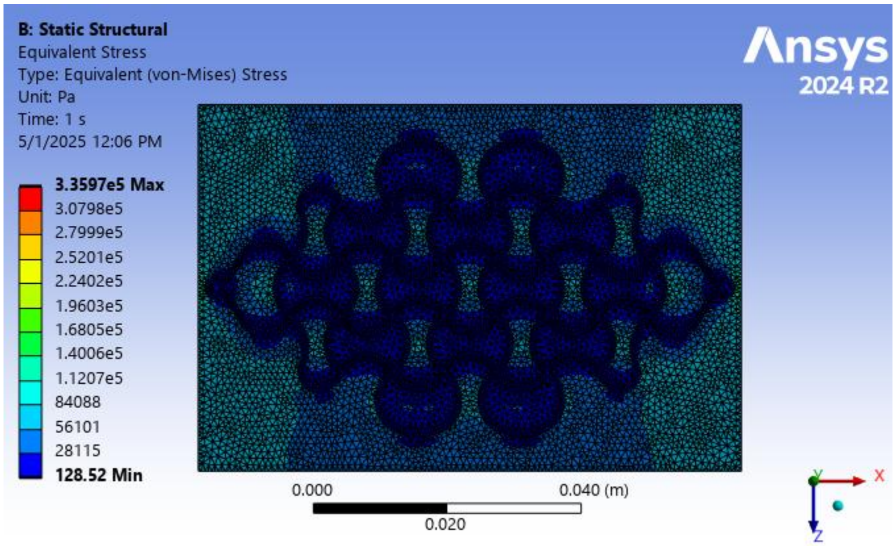

Figure 11. Equivalent (von Mises) stress results for biaxial stretching of PDMS substrate with CNT device.

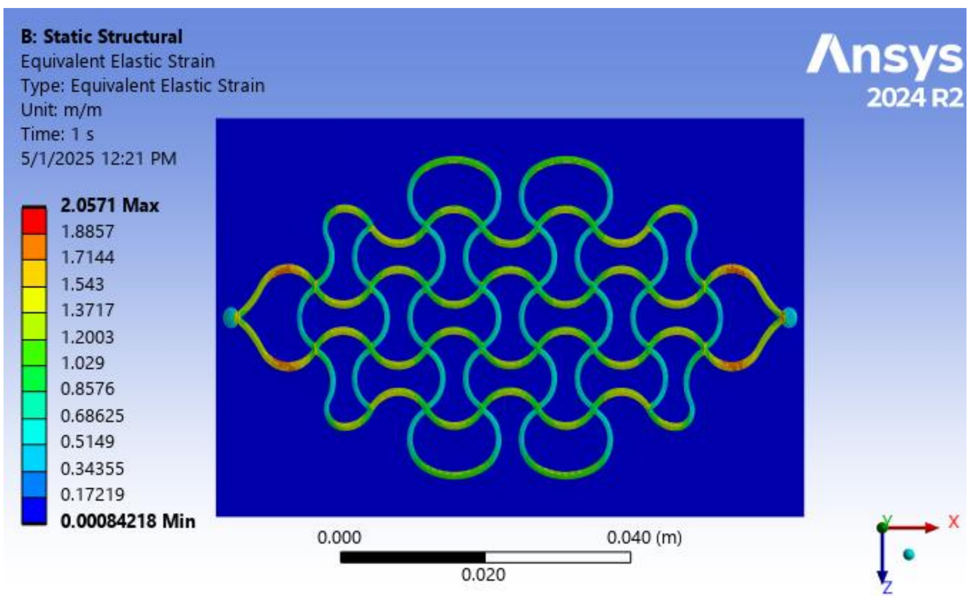

Figure 12. Equivalent elastic strain results for biaxial stretching of PDMS substrate and CNT device.

With cuts added to improve the stretchability of the sensor, identical displacements were again applied as in the model with no cuts. With this simulation, the maximum stress was located at the edges of the sensor, and the magnitude of that stress was slightly lower than the magnitude of stress without the kirigami cuts (see Figure 13).

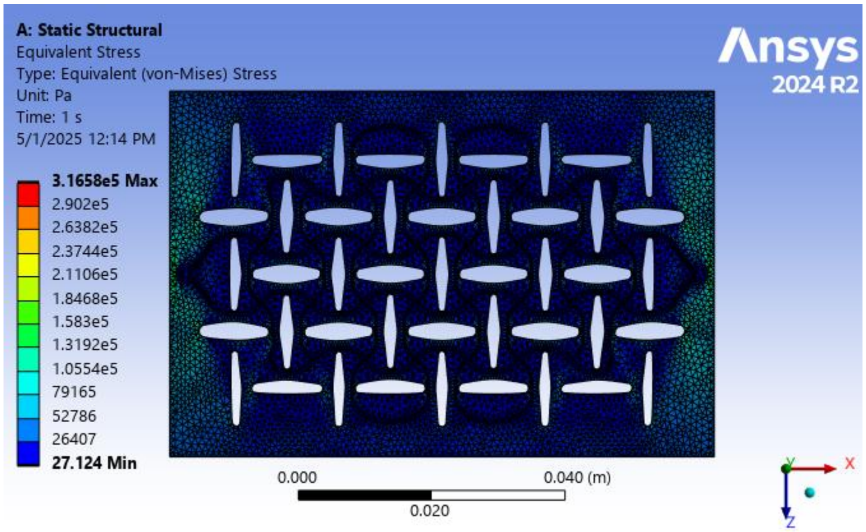

Figure 13. Equivalent von Mises stress for biaxial stretching of sensor with kirigami cuts incorporated.

For the strain in the sensor, the Ansys analysis showed the strain to be somewhat lower, although it was still located in the CNT/PDMS device (conductive ink) as shown in Figure 14.

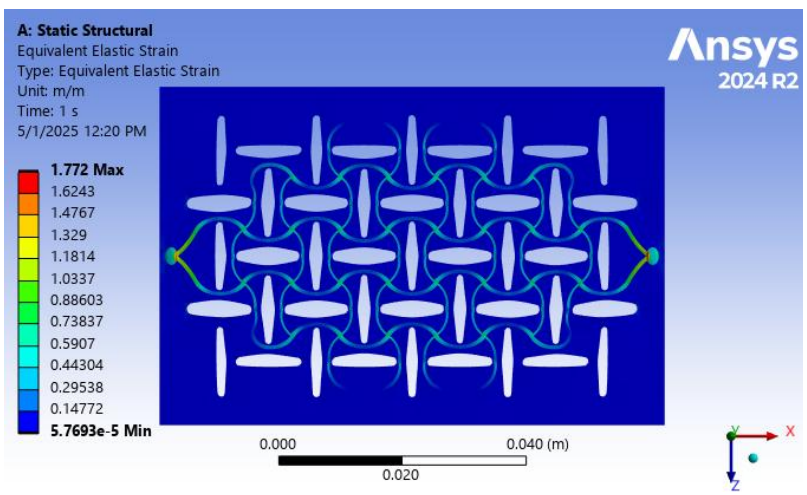

Figure 14. Equivalent elastic strain for biaxial stretching of sensor with kirigami cuts incorporated.

In the second test of our proposed kirigami design, a window cling vinyl was used as a substitute substrate to test the effectiveness of square- versus round-edged kirigami cuts. The vinyl was selected because it has a similar thickness and elasticity to the PDMS. A Cricut Cutter was used to incise the kirigami cuts into the vinyl. Each type of cut was stretched 10% of its original length to look for tearing and plastic deformation, as seen in Figures 15 and 16. The rounded cuts showed less deformation at 10% than the rectangular cuts.

Figure 15. Large scale prototype stretching of rounded kirigami substrate to 10% deflection.

Figure 16. Large scale prototype stretching of rectangular kirigami substrate to 10% deflection.

Testing

Prototyping and Manufacturing

The design and manufacturing of our strain-insensitive temperature sensor involves a molding and ink injection process utilizing polydimethylsiloxane (PDMS) and carbon nanotube

(CNT) composites. The device features a three-layered structure including a base layer of PDMS (mixed in a 10:1 ratio with curing agent); a middle layer composed of a CNT-PDMS mixture (mixed in a ratio of 2:1 PDMS to CNT) patterned in a sinusoidal and kirigami-cut design; and a final top layer of pure PDMS (also in 10:1 ratio with curing agent). This design strategically places the CNT layer along the neutral axis to minimize strain-induced resistance changes, allowing for a focus on temperature-dependent resistance variations only. Drawings for this design can be found in Appendix B.

Initially, laser cutting of PDMS was considered for creating the channels for the CNT ink. Unfortunately, the challenges in file compatibility between the design program and our laser-cutting machines led to the development of a molding-based approach only. This involved creating a two-part 3D printed mold to define the kirigami cuts and the channels for CNT ink injection (see Figure 17). Drawings for the 3D mold are also found in Appendix B.

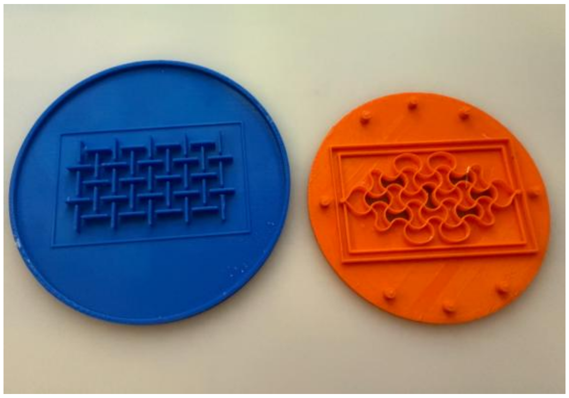

Figure 17. 3D printed mold. Bottom portion, on the left, has kirigami structure. Top portion, on right, has a design for sinusoidal channels into which conductive ink is injected.

The preparation of the PDMS base layers involves mixing PDMS base and curing agent (10:1 ratio) with up to 20% hexane to reduce viscosity, allowing better spreading of the polymer across our mold. A release spray is applied to the mold surfaces with a 5-minute waiting period before pouring the PDMS mixture. A 48-hour curing period is required before the PDMS can be demolded. After demolding, raised portions corresponding to the top mold are carefully shaved down to ensure uniform channel access for injection of conductive ink (Figure 18).

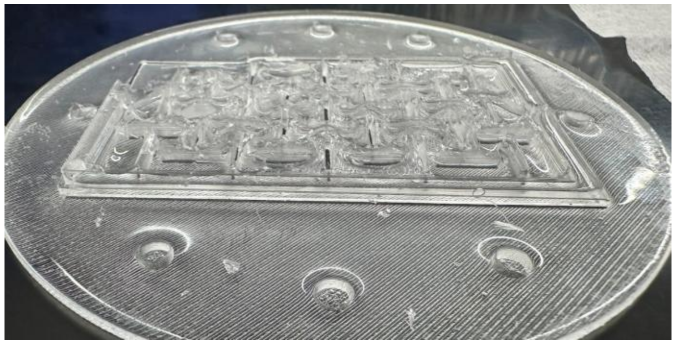

Figure 18. Demolded base substrate showing raised portions that needed to be shaved down.

The conductive CNT ink is formulated by combining PDMS base and CNTs in a 2 to 1 ratio, followed by the addition of hexane to a total volume of approximately 15 mL. This solution is then placed in an ultrasonic cleaner for 3 to 4 hours to ensure proper dispersion of the CNTs. Due to the ultrasonic cleaner's 100-minute cycle limit, continuous monitoring and restarting were necessary by members of the group throughout the mixing period. After this process, a curing agent and a cure accelerator, both in a 10:1 ratio to the PDMS base, are added to the CNT mixture. This ink is then injected into the channels within the molded PDMS structure and allowed to cure for a minimum of 10 hours.

Prior to applying the top PDMS layer, silver epoxy was carefully applied to the ink channel ends, extending roughly a quarter inch upwards to serve as conductive contacts for testing or device manufacturing. The process for creating the base PDMS layer is then repeated to form the top layer, ensuring proper alignment with the bottom mold. A minimum 48 hour curing period is required before the completed sensor can be removed from the mold and trimmed to the final dimensions using scissors.

The significant time investment associated with PDMS curing, mixing in the ultrasonic cleaner, and meticulous mold preparation presented key technical challenges in the manufacturing process. The sensitivity of PDMS to tearing or being improperly cured at the time of demolding also necessitated careful handling and the use of release sprays.

Uniaxial and Biaxial Loading

The initial phase of mechanical testing focused on determining the optimal ratio of PDMS base to curing agent that would provide a suitable balance of mechanical properties for the sensor to be applied to human skin. We aimed for a material that was neither overly brittle nor excessively ductile. To this end, uniaxial tensile tests were performed on PDMS samples prepared with varying agent ratios using a Biotester. Force and displacement data were recorded during these tests, allowing for the generation of stress-strain curves for each ratio.

The evaluation of the mechanical properties was primarily based on a visual assessment of the resulting stress-strain curves. Our goal was to identify a ratio that exhibited sufficient elasticity without premature failure under strain, a balance of ductility, and brittleness. The 10:1 PDMS base-to-curing agent ratio demonstrated the most promising balance, exhibiting a suitable level of flexibility without indications of premature failure (see Figure 19).

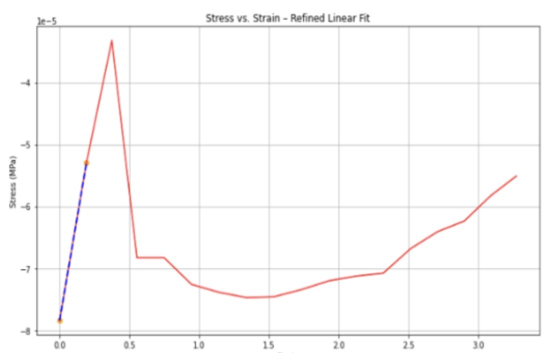

Figure 19. Stress-strain curve for 10:1 PDMS mixture. Young’s modulus is shown to be 1.3229 MPa.

To isolate the mechanical impact of the kirigami cuts, uniaxial tensile tests were also conducted on PDMS samples prepared with the 10:1 ratio, both with and without the incorporated kirigami cut patterns. These tests, conducted on samples without the conductive CNT ink, allowed us to assess how the cuts themselves affected the uniaxial mechanical response of the PDMS base material.

Recognizing that real-world applications often involve complex, multi-axial stress states, we also performed biaxial tensile testing on samples with the 10:1 PDMS ratio and the kirigami cut design using the Biotester. Biaxial testing provides a more realistic simulation of the forces and deformations the sensor might experience in operation compared to uniaxial testing.

The mechanical response of the kirigami structure under biaxial loading proved to be more complex than conventional uniaxial material behavior and took trial and error with the limited research on this topic. As anticipated, the force-displacement relationship did not follow a simple superposition of uniaxial responses due to the geometry and deformation mechanisms of the kirigami cuts. Initial biaxial tests where one direction of tension was dominant resulted in the greatest displacement occurring in that direction.

Crucially, observations during biaxial testing revealed the deformation behavior of the kirigami cuts. Under biaxial strain, the cuts were observed to open, allowing for expansion of the sensor in multiple directions. However, these tests also indicated potential failure points, particularly at any corners of the kirigami patterns, which appeared susceptible to tearing under biaxial stress, and were a result of the molding process' limited level of precision.

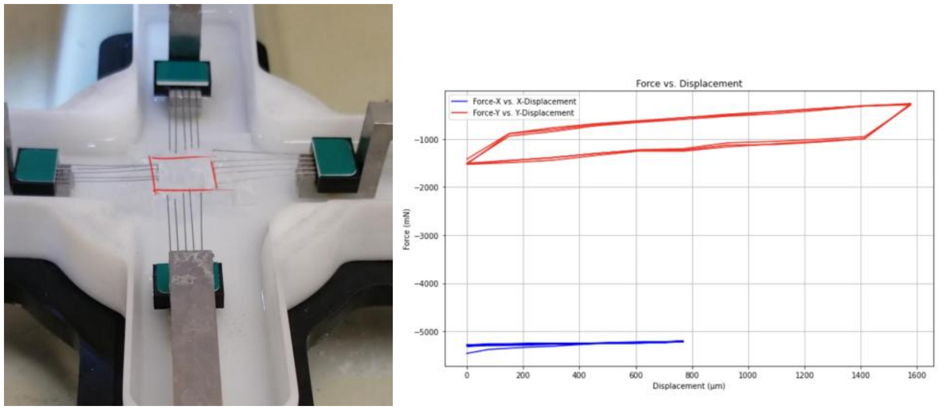

Figure 20. On the left, a kirigami PDMS substrate placed in the Biotester device. PDMS outlined in red due to the transparent nature of the material. On the right is a force vs. displacement curve for kirigami PDMS substrate.

Resistance Testing: Temperature and Curvature

The initial prototype that we developed featured a ratio of PDMS to CNTs of 10 to 1. Testing of this device showed that there was no conductivity in the device and we were able to conclude that the ratio of CNTs to PDMS was not high enough to ensure conductivity. Due to constraints on time, especially the amount of time to make a new prototype, we opted to make a conductive ink with a ratio of 2 to 1 of PDMS to CNTs. With this ratio, we were able to detect resistance in the sensor and moved on to testing for resistance versus temperature when the sensor was placed on a flat surface.

For this test, leads were connected to the silver epoxy at each end of the sensor by applying more silver epoxy around the leads. Then copper conductive tape was used to tape the leads and silver epoxy in a more stable manner (see Figure 21). Finally, the free ends of the leads were taped to the leads of a digital multimeter (DMM) with more copper conductive tape.

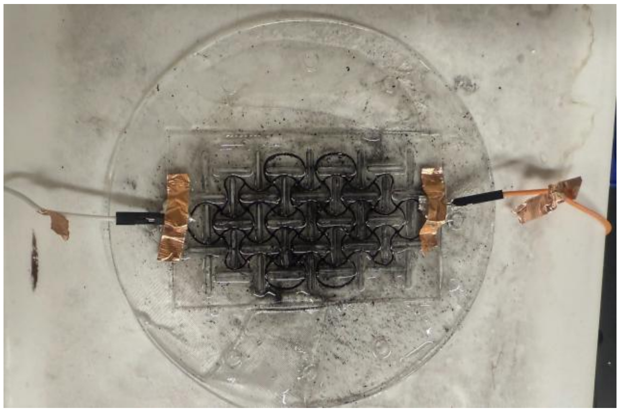

Figure 21. Flexible temperature sensor prepared for testing with DMM.

To test the ways in which resistance changes in reaction to changes in temperature, the sensor was placed on the surface of a heater with precise temperature controls. Initially, the heater was set to 30º C and we waited four minutes before testing resistance in the sensor. Temperature for the heater was then raised by 1 degree and we waited four minutes between each raising of the temperature to attempt to let the device reach steady state before testing resistance. The results of our testing from 30º C to 45º C can be seen in Figure 22. As is shown, the resistance initially became lower with each incremental rise in temperature, as was expected. However, around 35º C, the resistance measured did not change much between 35º C and 41º C, at which point the resistance jumped higher at 42º C before resuming its downward trend between 42º C and 45º C. We expected a linear trend, but did not see that in our testing, as shown by the R^2 value of only 0.364.

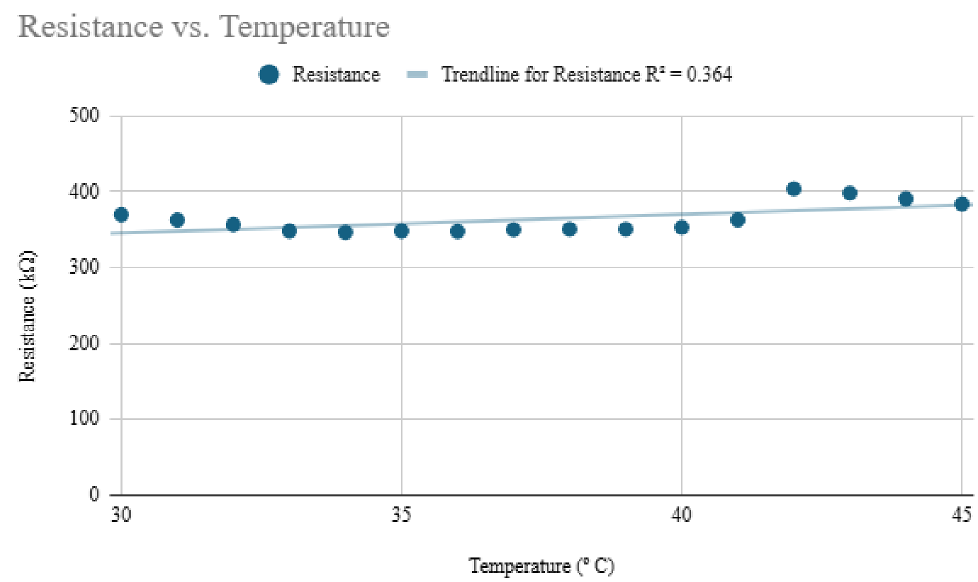

Figure 22. Resistance vs. Temperature for temperature range from 30º C to 45º C. Linear trendline shown with associated R^2 value of 0.364.

After testing resistance at different temperatures for the sensor, the sensor was then placed on a flat surface at room temperature and a resistance of 362.2 kΩ was measured. Then the sensor was placed on a curved surface, with the shorter side of the sensor along the curve, and the resistance was measured again. The resistance on the curved surface was 382.9 kΩ, which is an increase of 5.7%. The sensor was then placed so the longer side of the sensor was along the curve and resistance was measured as 474.1 kΩ, which is an increase of 30.9%. This shows that the kirigami structure may help to alleviate changes in resistance due to strain, but possibly only when the sensor is subjected to strain along its shorter dimension.

Summary and Conclusions

Our graph for temperature vs. resistance did not produce the results we were searching for. Possible reasons for this are likely tied to our manufacturing process and possibly to the ratio of CNTs to PDMS used for the conductive ink for the device. The initial ratio of 10:1 that had no conductivity showed a high dependence on the ratio chosen. When the DMM was connected to our sensor, we had to wait several minutes before the resistance being measured seemed to stop changing. This was likely due to the very small current that the DMM used which might have heated the CNTs up and changed the resistance in the ink. A smaller ratio of CNTs to PDMS might have helped to alleviate the changes in resistance seen due to the DMM being used.

For the manufacturing process, using a laser to cut the channels for the CNTs might have resulted in a more uniform top surface for the sensor. Another option that could have been pursued using the laser, would have been to set the strength of the laser so that when the channels are cut for the location of the device, black carbon would be left in the channels which would then be able to serve as the conductive device without further addition of CNTs by a manual process. Cutting the kirigami design at the same time would allow for even further precision in the manufacturing of the device.

Further testing is needed to determine if the kirigami structure is indeed helping alleviate resistance changes due to strain. Testing of a prototype with no kirigami structure would need to be performed in order to make a comparison. Flexibility of the device is also a factor in the testing of the kirigami structure and a thinner sensor would be more flexible so that the sensor will bend easily on its own around different curvatures.

Appendix A

References

CellScale - BioTester - Biaxial testing for soft materials. (2016, November 10). CellScale. https://www.cellscale.com/products-cellscale-biomaterials-testing/biotester/

Commissioner, O. of the. (2017, September 27). *FDA approves first continuous glucose monitoring system for adults not requiring blood sample calibration*. FDA. https://www.fda.gov/news-events/press-announcements/fda-approves-first-continuous-glucose-monitoring-system-adults-not-requiring-blood-sample

Nag, A., Mukhopadhyay, S., & Kosel, J. (2017, May 18). *Wearable Flexible Sensors: A Review*. IEEE Xplore. https://ieeexplore.ieee.org/abstract/document/7931559/authors#authors

Van Beers, C., & DeVries, J. H. (2015). Analysis: The Accuracy and Efficacy of the Dexcom G4 Platinum Continuous Glucose Monitoring System. *Journal of Diabetes Science and Technology*, *9*(5). Sage Journals.

Won, P., Jung Tak Park, Lee, T., Ha, I., Han, S., Choi, M., Lee, J., Hong, S., Cho, K.-J., & Seung Hwan Ko. (2019). Stretchable and Transparent Kirigami Conductor of Nanowire Percolation Network for Electronic Skin Applications. *Nano Letters, 19*(9), 6087–6096. https://doi.org/10.1021/acs.nanolett.9b02014

Yu, M., et al. (2022). A flexible dual-mode pressure sensor for wearable electronics. *Nature Communications, 13*(1), 18321. https://doi.org/10.1038/s41598-022-18321-6

Appendix B

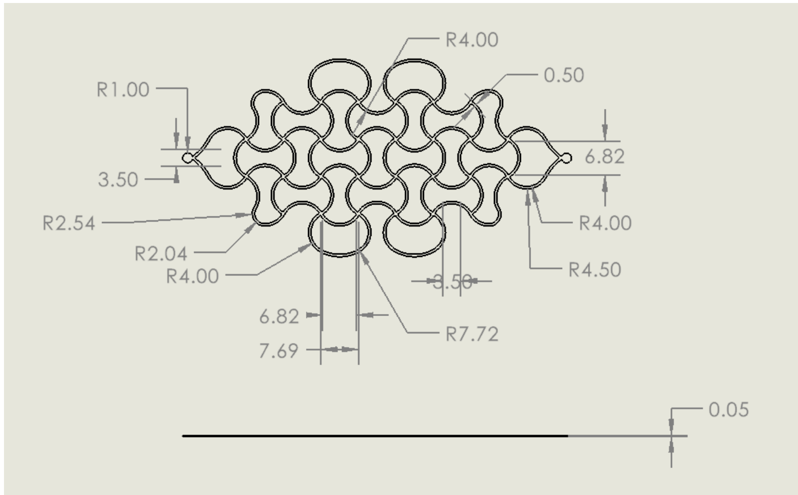

Figure 23: Drawing of conductive ink (device). Dimensions in mm.

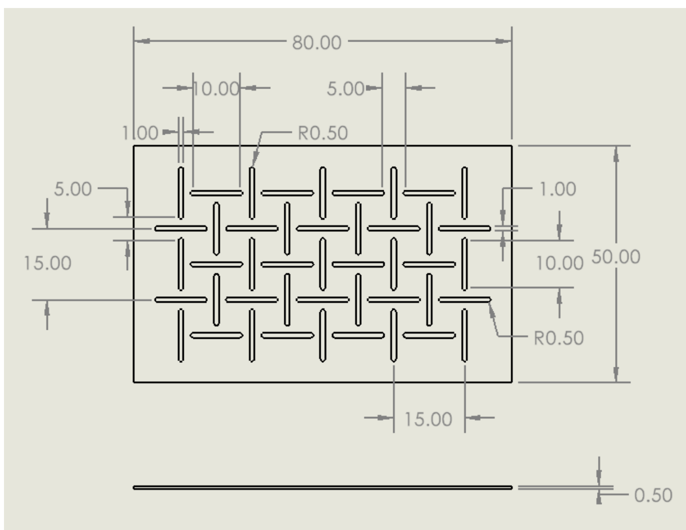

Figure 24: Drawing of substrate layer and protective top layer (identical to each other). Dimensions in mm.

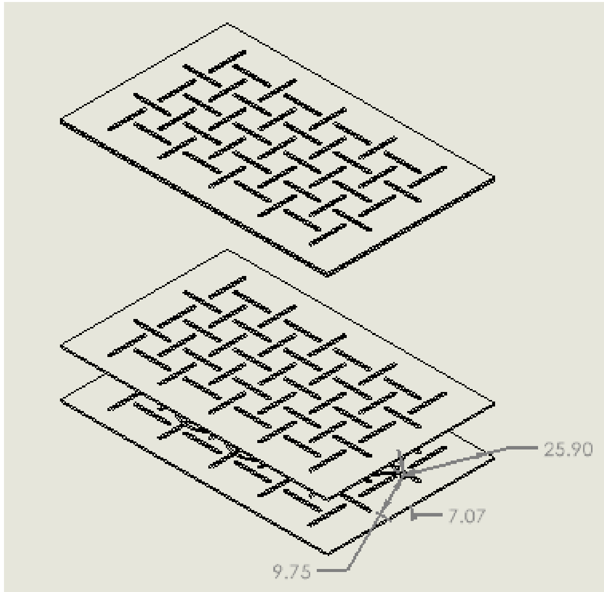

Figure 25: Drawing of assembly with substrate layer, device, and top layer. Device is centered on the substrate layer. Dimensions in mm.

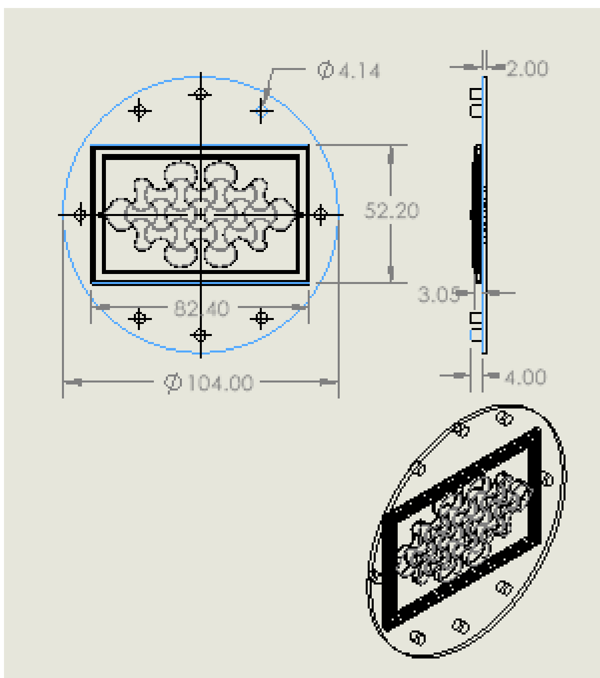

Figure 26: Drawing of top portion of 3D mold. Dimensions in mm.

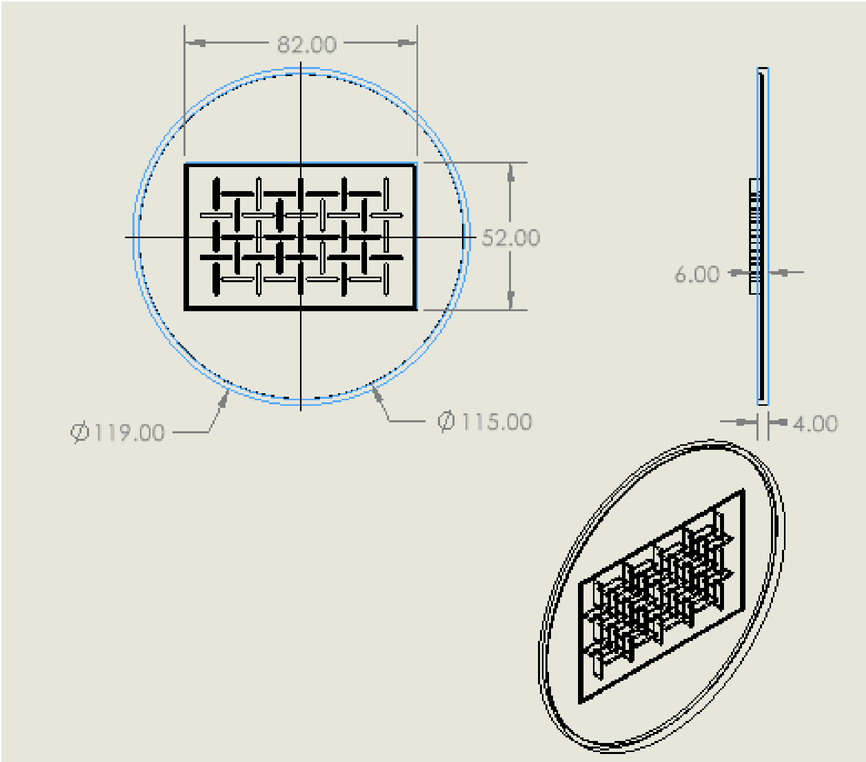

Figure 27: Drawing of bottom portion of 3D mold. Dimensions in mm.

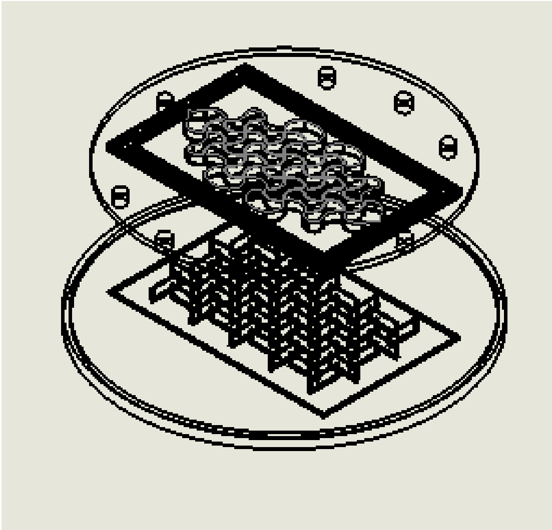

Figure 28: Drawing of 3D mold assembly.

Appendix C

Bill of Materials

Part Number	Part Name	Size	Quantity	Cost Per Item	Shipping Cost	Total Cost
1	Sylgard 184 Elastomer (PDMS)	0.5 kg	2	156.16	9.25	321.57
2	MWNT-COOH (98%, OD 5-15nm)	5 g	1	85.00	25.00	110.00
3	Hexane	1 L	1	141.00		141.00
4	Silver Conductive Epoxy	0.52 oz	1	128.94	6.99	135.93
5	Sterilized Petri Dishes (pack of 20)	15 cm	3	21.99		65.97
6	Centrifuge Tubes (pack of 25)	50 mL	2	16.99		33.98
7	Copper Foil Tape with Conductive Adhesive	25 mm x 82.5 ft	1	12.59		12.59
8	3-D Printed Parts	Various	1	41.74		41.74
Total						862.78